Direction-of-Arrival Estimation Exploiting Distributed Sparse Arrays

Md. Waqeeb T. S. Chowdhury and Yimin D. Zhang

Department of Electrical and Computer Engineering, Temple University, Philadelphia, PA 19122, USA

Abstract—**In this paper, we present a novel direction-of-arrival (DOA) estimation strategy that exploits distributed sparse sensor arrays and structured matrix completion-based information fusion techniques to provide superior DOA estimation performance with enhanced degrees-of-freedom. We consider a sparse array consisting of a plurality of distributed subarrays such that each subarray is calibrated, whereas the inter-subarray spacing is unknown. The subarrays are designed to collectively offer difference lags with minimum redundancy, and the received data matrix obtained from distributed subarrays are fused by exploiting structured matrix completion, resulting in enhanced degrees-of-freedom and improved DOA estimation performance. The proposed strategy is able to resolve more sources than the total number of available sensors. Simulation results illustrate the performance of the proposed strategy.**

Keywords: Direction-of-arrival estimation, distributed sensor array, partially calibrated array, non-coherent processing, structured matrix completion, degrees-of-freedom.

I. Introduction

In array signal proce1sing, direction-of-arrival (DOA) estimation is one of the most important technologies that find wide applications in the fields of radar, sonar, wireless communications, and radio astronomy [1, 2]. Due to the Nyquist sampling theorem, uniform linear arrays (ULAs) have traditionally considered as the commonly used sensor array structure for DOA estimation and its performance has been well analyzed [1–4]. However, ULAs are not efficient in terms of their aperture and the offered degrees-of-freedom (DOFs). In particular, they cannot resolve more sources than the number of array elements using second-order statistics. Several research efforts have been made in the past to detect more sources than the number of sensors using sparse arrays by exploiting their difference co-arrays [5–8]. This resulted in the development of classical sparse array structures like minimum redundancy array (MRA) [5] and the minimum hole array (MHA) [7, 8].

Recently, significant research efforts have been dedicated to develop systematical sparse array designs which follow a specific design formulation or structure, thus enabling convenient design and analysis. In this context, two notable sparse arrays are the nested array [9] and the coprime array [10]. These array structures and their variants have been extensively analyzed, and closed-form expressions for their design process and the achievable number of DOFs are devised [9–14]. Structured sparse array design and analysis exploiting higher-order statistics [15–17] and frequency diversity [18–24] have also attracted significant attention. Recently developed compressive sensing-based DOA estimation methods enable sparse arrays to effectively use all the co-array lags for DOA estimation [11, 12, 25, 26]. In addition, exploiting Toeplitz structure-based covariance matrix interpolation strategies [8, 27–30] can further provide higher estimation accuracy.

When forming a large-size array is not feasible, an attractive alternative is to exploit distributed arrays, which consist of multiple separately spaced array platforms. Such configurations are useful in, e.g., distributed unmanned aerial vehicles (UAVs) and unmanned underwater vehicles (UUVs), where each vehicle is equipped with a small number of antennas or hydrophones. In such platforms, comparing to distributed arrays processed individually, fusion of their information received at all subarrays provides additional benefits.

Data processing performed at a distributed array system can be broadly classified into two types, namely, coherent processing and non-coherent processing. In non-coherent processing, the covariance matrix of each subarray is computed locally, and these individual covariance matrices are then transmitted to a fusion center so that they are joint exploited to resolve the source directions [31]. Non-coherent processing is considered in this paper due to its practical feasibility. The mobility of distributed subarrays often renders coherent processing challenging due to the uncertainty in the inter-subarray spacing and sampling time of the individual systems. Coherent processing also requires that raw data are transferred to the fusion center.

In this paper, we consider a distributed sparse array system consisting of partly calibrated distributed subarrays. The subarrays are co-located in the sense that all subarrays share the same DOA observation for each of the sources. Each subarray is calibrated such that we know the location and the gain/phase of each sensor in a subarray with reference to the first sensor of the corresponding subarray. However, the relative distance between the distributed subarrays is considered unknown. As such, the subarray signals are fused in a non-coherent manner. It will be shown in this paper that distributed arrays not only increase the number of DOFs for a given number of sensors at each subarray, but also provide increased maneuverability. We also address the provision of incorporating the concept of information fusion from multiple array platforms and utilize structured array interpolation techniques to significantly enhance the performance of such distributed systems.

The rest of the paper is organized as follows. The signal model of distributed sparse arrays is described in Section II. In Section III, we present the proposed information fusion technique exploiting structured matrix interpolation to achieve DOF enhancement. A numerical example is provided in Section IV to demonstrate the effectiveness of the proposed method. Finally, conclusions are drawn in Section V.

Notations: We use lower-case (upper-case) bold characters to denote vectors (matrices). In particular, $\mathbf{I}_N$ denotes the $N \times N$ identity matrix. $(.)^{\mathrm{T}}$ and $(.)^{\mathrm{H}}$ respectively represent the transpose and conjugate transpose of a matrix or a vector. In addition, $|\cdot|_F$ denote the Frobenius norm, $\circ$ is the Hadamard product operator, $\mathcal{T}(\boldsymbol{x})$ denotes the Hermitian-Toeplitz matrix with $\boldsymbol{x}$ as its first column, and $\mathrm{Tr}(\cdot)$ represents the trace operator. Furthermore, $[\mathbf{A}]_{u,v}$ denotes the (u, v)th element of matrix $\mathbf{A}$, and $\mathbb{E}[\cdot]$ is the statistical expectation operator.

II. System Model

Consider a distributed sparse sensor array system consisting of K distributed sparse linear subarrays such that each subarray is equipped with M sensors. The sensor locations of the kth subarray with respect to their first (reference) sensor are denoted by the following position set:

$$\mathbb{S}_k = \{0, p_{2,k}d, \ldots, p_{M,k}d\}, \quad k = 1, \ldots, K, \tag{1}$$

where $p_{m,k}d$, $m = 1, \ldots, M$, denotes the distance between the first and the mth sensors in the kth subarray, $d = \lambda/2$, and λ denotes the wavelength of the impinging signals. The physical distance between the reference sensor of the k_1th subarray and the reference sensor of the k_2th subarray, denoted as $D_{k_1k_2}$, where $k_1, k_2 = 1, \ldots, K$ and $k_1 \neq k_2$, is assumed unknown.

Consider L uncorrelated far-field narrow-band signals impinging on all K subarrays from distinct angles $\{\theta_1, \cdots, \theta_L\}$. It is assumed that all subarrays observe the same angle for each source. The baseband signal vector $\mathbf{x}_k(t)$ received at the kth sparse subarray is expressed as:

$$\begin{aligned}\mathbf{x}_k(t) &= \sum_{l=1}^{L} \rho_k \mathbf{a}_k(\theta_l) s_l(t) + \mathbf{n}_k(t) \\ &= \rho_k \mathbf{A}_k \mathbf{s}(t) + \mathbf{n}_k(t), \quad k = 1, \ldots, K,\end{aligned} \tag{2}$$

where ρ_k denotes the phase shift at kth subarray due to the physical distance between each other, $s_l(t)$ denotes the signal waveform impinging from direction θ_l, and $\mathbf{s}(t) = [s_1(t), \cdots, s_L(t)]^{\mathrm{T}}$. In addition, the vector

$$\mathbf{a}_k(\theta) = [1, e^{-j\frac{2\pi p_{2,k} d}{\lambda}\sin(\theta)}, \ldots e^{-j\frac{2\pi p_{M,k} d}{\lambda}\sin(\theta)}]^{\mathrm{T}} \tag{3}$$

denotes the steering vector of the kth subarray for the signal impinging from angle θ, and $\mathbf{n}_k(t)$ denotes the additive circularly complex white Gaussian noise vector observed at the kth subarray. The array manifold $\mathbf{A}_k$ corresponding to the kth subarray is given as:

$$\mathbf{A}_k = [\mathbf{a}_k(\theta_1), \mathbf{a}_k(\theta_2), \ldots, \mathbf{a}_k(\theta_L)], \quad k = 1, \ldots, K. \tag{4}$$

The covariance matrix of the received data for the kth subarray is given as:

$$\begin{aligned}\mathbf{R}_k &= \mathbb{E}[\mathbf{x}_k(t)\mathbf{x}_k^{\mathrm{H}}(t)] = \mathbf{A}_k \mathbf{S} \mathbf{A}_k^{\mathrm{H}} + \sigma_{\mathrm{n},k}^2 \mathbf{I}_M \\ &= \sum_{l=1}^{L} \sigma_l^2 \mathbf{a}_k(\theta_l)\mathbf{a}_k^{\mathrm{H}}(\theta_l) + \sigma_{\mathrm{n},k}^2 \mathbf{I}_M, \quad k = 1, \ldots, K,\end{aligned} \tag{5}$$

where $\sigma_{\mathrm{n},k}^2$ denotes the noise power at the kth subarray and $\mathbf{S} = \mathbb{E}[\mathbf{s}(t)\mathbf{s}^{\mathrm{H}}(t)] = \mathrm{diag}([\sigma_1^2, \sigma_2^2, \cdots, \sigma_L^2])$ is the source covariance matrix with σ_l^2 denoting the power of the lth source, $l = 1, \ldots, L$. In pactice, the covariance matrix can be estimated using the sampled data at each subarray, i.e.,

$$\hat{\mathbf{R}}_k = \frac{1}{N_k} \sum_{t=1}^{N_k} \mathbf{x}_k(t)\mathbf{x}_k^{\mathrm{H}}(t), \quad k = 1, \ldots, K, \tag{6}$$

where N_k is the number of snapshots available at the kth subarray. For simplicity, we assume that the same number of snapshots, N_k, is received at each subarray.

III. DOA Estimation Exploiting Information Fusion and Covariance Matrix Interpolation

In this paper, we aim to resolve the maximum number of spatial sources using a partly calibrated distributed array via non-coherent processing. A total covariance matrix is reformulated at the fusion center and includes the covariance matrix entries from all subarrays. The resulting total covariance matrix is generally a sparse matrix when the subarrays are designed to explore the full potential of distributed sparse arrays. In this case, we exploit the concept of structured matrix completion to interpolate the full entries of the sparse covariance matrix [22, 27, 30]. The interpolated total covariance matrix enables gridless DOA estimation, provides more robust DOA estimation performance, and achieves a higher number of DOFs to enable estimation of more sources than the total number of sensors in all the subarray platforms combined. The proposed scheme is described in the following two subsections.

A. Information Fusion

Since we consider non-coherent processing for the underlying partly calibrated distributed array system, we compute the local covariance matrix at each subarray as shown in (6). The fusion center receives K different covariance matrices and performs fusion with these covariance matrices. Note that the dimension of the total covariance matrix $\hat{\mathbf{R}}$ is determined by the maximum aperture of the subarrays $Pd = \max_k(p_{M,k})d$ and is given as $(P + 1) \times (P + 1)$.

When matrix $\hat{\mathbf{R}}$ is sparse, that is, it contains missing entries, it is effective to perform matrix completion to interpolate these missing entries. Such matrix completion can exploit the Hermitian and Toeplitz structure of the total covariance matrix when it is fully interpolated [22, 27, 30]. This is described in the following subsection.

B. Covariance Matrix Interpolation

Since this paper encompasses the non-coherent processing for the data observed at multiple subarrays, each subarray transmit their locally computed covariance matrix to the fusion center. The fusion center performs the processing with the received K sets of covariance matrices as described below.

We first define a binary vector b_k to indicate whether a sensor at position ld is present in the kth subarray $\mathbb{S}_k$, i.e.,

$$\langle \mathbf{b}_k \rangle_l = \begin{cases} 1, & ld \in \mathbb{S}_k, \\ 0, & \text{otherwise.} \end{cases} \tag{7}$$

where l is the index of the sensor location with $l \in [0, \cdots, P]$ and $\langle \cdot \rangle_l$ denotes the element corresponding to the sensor position at ld. We also define $\mathbf{B}_k = \mathbf{b}_k(\mathbf{b}_k)^{\mathrm{T}}$, shown in Fig. 2 as the binary mask matrix with unit-valued entries representing observed elements in $\hat{\mathbf{R}}_k$. In the binary mask shown in Fig. 2, the blue, yellow and orange entries correspond to the self lag positions due to $\mathbb{S}_1$, $\mathbb{S}_2$ and $\mathbb{S}_3$ respectively.

The total synthesized covariance matrix corresponding to the K subarrays are given as,

$$\hat{\mathbf{R}} = \left(\sum_{k=1}^{K} \hat{\mathbf{R}}_k \circ \mathbf{B}_k \right) \circ \mathbf{D}, \tag{8}$$

where matrix $\mathbf{D}$ averages the redundant lag entries in $\hat{\mathbf{R}}_k$. The (u, v)th element of matrix $\mathbf{D}$ is given as

$$[\mathbf{D}]_{u,v} = \frac{1}{\sum_{i=1}^{K} [\mathbf{B}]_{u,v} + \epsilon}, \tag{9}$$

with ϵ denoting a small positive value in order to provide stability of the division.

It is noted that conventional matrix completion may often fail to interpolate the missing elements of $\hat{\mathbf{R}}$ because some rows or columns are completely missing. In this case, the reconstructability can be improved by taking the Hermitian and Toeplitz structure of the full covariance matrix into account, thereby yielding structured matrix completion. The matrix recovery problem can be formulated as the following low-rank structured matrix completion problem:

$$\begin{aligned} \min_{\boldsymbol{\omega}} \quad & \operatorname{rank}(\mathcal{T}(\boldsymbol{\omega})) \\ \text{s.t.} \quad & \|\mathcal{T}(\boldsymbol{\omega})\mathbf{B} - \hat{\mathbf{R}}\|_F^2 \leq \delta, \\ & \mathcal{T}(\boldsymbol{\omega}) \succcurlyeq 0, \end{aligned} \tag{10}$$

where δ is a parameter indicating error tolerance. Because the rank minimization problem is NP-hard, this problem is relaxed to the following nuclear norm minimization:

$$\begin{aligned} \min_{\boldsymbol{\omega}} \quad & \|\mathcal{T}(\boldsymbol{\omega})\mathbf{B} - \hat{\mathbf{R}}\|_F^2 + \zeta \mathbf{Tr}\left(\sqrt{\mathcal{T}^{\mathrm{H}}(\boldsymbol{\omega})\mathcal{T}(\boldsymbol{\omega})} \right), \\ \text{s.t.} \quad & \mathcal{T}(\boldsymbol{\omega}) \succcurlyeq 0, \end{aligned} \tag{11}$$

where $\|\mathcal{T}(\boldsymbol{\omega})\|_* = \mathbf{Tr}(\sqrt{\mathcal{T}^{\mathrm{H}}(\boldsymbol{\omega})\mathcal{T}(\boldsymbol{\omega})})$ represents the nuclear norm of $\mathcal{T}(\boldsymbol{\omega})$, and ζ is a tunable regularization parameter. It usually takes a larger value when the number of sources to be resolved is higher.

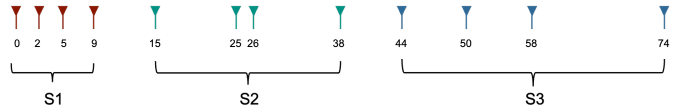

Fig. 1: Distributed array configuration.

IV. Numerical Results

We consider a sparse array system consisting of 3 spatially distributed subarrays located in a collinear fashion, and each subarray consists of 4 omni-directional sensors, rendering the total number of 12 sensors as shown in Fig. 1. $L = 17$ uncorrelated sources are assumed to be uniformly distributed between $[-60°, 60°]$.

The array locations for each subarray are given as follows:

$$\begin{aligned} \mathbb{S}_1 &= \{0, 2, 5, 9\}d, \\ \mathbb{S}_2 &= \{15, 25, 26, 38\}d, \\ \mathbb{S}_3 &= \{44, 50, 58, 74\}d. \end{aligned}$$

The largest subarray has an aperture of $Pd = 31d$. We consider 500 data snapshots at each subarray whereas the input signal-to-noise ratio (SNR) is 0 dB.

Fig. 2 shows the binary mask indicating the positions of the observed covariance matrix entries. Fig. 3(a) shows the superposition of all difference lags computed from each subarray. It is noted that the difference lags do not count for the cross-lags between different subarrays due to the non-coherent processing. It is confirmed that the subarray configurations are designed in such a way that the maximum number of unique lags are achieved with no redundancies except at lag zero.

The structure matrix completion reconstruct the 31×31 total covariance matrix so that all 17 sources are resolved with a high resolution, as we can verify from the MUSIC pseudo-spectrum depicted in Fig. 3(b). For comparison, Fig. 3(c)

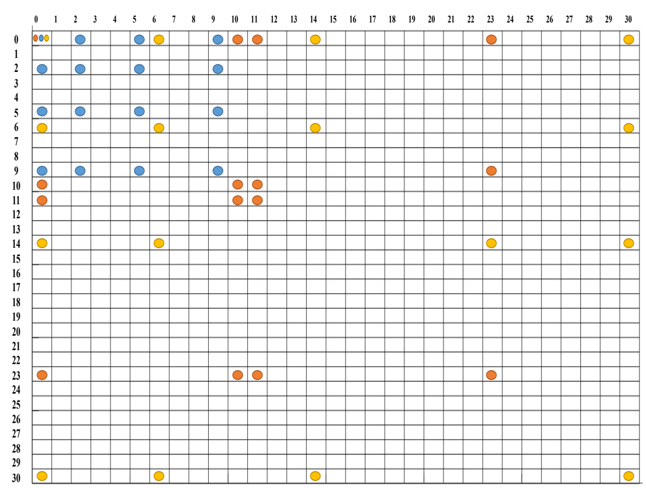

Fig. 2: Binary mask for covariance matrix interpolation at fusion center.

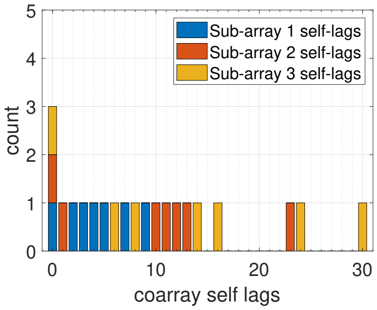

(a) Co-array self-lags offered by the covariance matrices of the three subarrays.

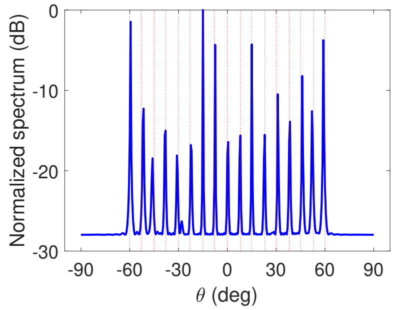

(b) All 17 sources are resolved after performing structured matrix completion.

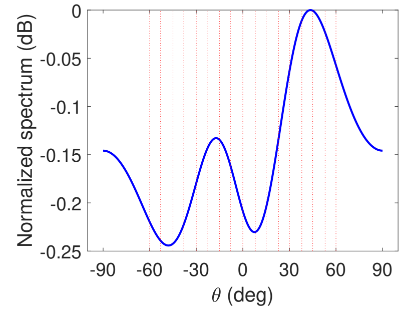

(c) The 17 sources are not resolved without performing matrix completion.

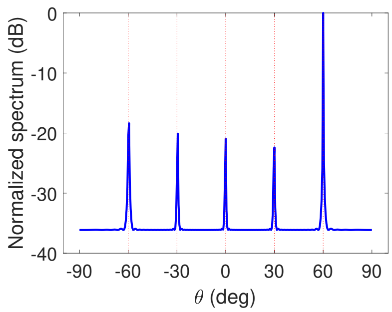

(d) 5 sources are clearly resolved after performing structured matrix completion.

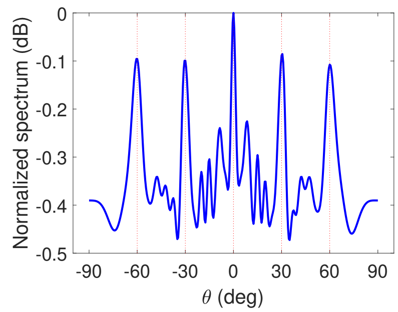

(e) Without performing matrix completion, 5 sources are resolved but with high sidelobes.

Fig. 3: Co-array configuration and DOA estimation performance.

shows the MUSIC pseudo-spectrum when MUSIC is directly applied to the total covariance matrix without performing structured matrix completion. As MUSIC assumes a full covariance matrix, its direct application to the covariance matrix is expected to have deteriorated DOA estimation performance. It is clear that MUSIC does not provide the enough DOFs to render meaningful DOA estimation performance.

To compare the MUSIC pseudo-spectra with and without structured matrix completion, we now consider a five-source scenario so that the number of sources is less than the total number of sensors. Comparing Fig. 3(d) and Fig. 3(e), it is observed that both cases result resolved MUSIC pseudo-spectra. However, the results obtained without performing structured matrix completion render low spatial resolution and high sidelobes.

V. Conclusion

This paper focuses on the design and processing of non-coherent distributed arrays to resolve a high number of sources which exceeds the total number of distributed sensors. Non-coherent processing only requires transmission of local covariance matrices for effective data fusion with minimum information exchange. Structured matrix completion is used to interpret the sparse total covariance matrix in the fusion center to enhance achieve a higher number of DOFs, and the effectiveness in achieving improved DOA estimation performance is clearly demonstrated using simulation results.

VI. References

[1] H. L. Van Trees, *Optimum Array Processing: Part IV of Detection, Estimation, and Modulation Theory*. John Wiley, 2002.

[2] T. E. Tuncer and B. Friedlander (Eds.), *Classical and Modern Direction-of-Arrival Estimation.* Elsevier, 2009.

[3] R. Schmidt, "Multiple emitter location and signal parameter estimation," *IEEE Trans. Antennas Propag.,* vol. 34, no. 3, pp. 276–280, March 1986.

[4] R. Roy and T. Kailath, "ESPRIT–Estimation of signal parameters via rotational invariance techniques," *IEEE Trans. Acoust., Speech, Signal Process.*, vol. 37, no. 7, pp. 984–995, July 1989.

[5] A. Moffet, "Minimum-redundancy linear arrays," *IEEE Trans. Antennas Propagat.*, vol. 16, no. 2, pp. 172–175, March 1968.

[6] R. T. Hoctor and S. A. Kassam, "The unifying role of the co-array in aperture synthesis for coherent and incoherent imaging," *Proc. IEEE*, vol. 78, no. 4, pp. 735–752, April 1990.

[7] E. Vertatschitsch and S. Haykin, "Nonredundant arrays," *Proc. IEEE*, vol. 74, no. 1, pp. 217–217, Jan. 1986.

[8] A. Ahmed and Y. D. Zhang, "Generalized non-redundant sparse array designs," *IEEE Trans. Signal Process.*, vol. 69, pp. 4580–4594, Aug. 2021.

[9] P. Pal and P. P. Vaidyanathan, "Nested arrays: A novel approach to array processing with enhanced degrees of freedom," *IEEE Trans. Signal Process.,* vol. 58, no. 8, pp. 4167–4181, Aug. 2010.

[10] P. P. Vaidyanathan and P. Pal, "Sparse sensing with co-prime samplers and arrays," *IEEE Trans. Signal Process.,* vol. 59, no. 2, pp. 573–586, Feb. 2011.

[11] S. Qin, Y. D. Zhang, and M. G. Amin, "Generalized coprime array configurations for direction-of-arrival estimation," *IEEE*

Trans. Signal Process., vol. 63, no. 6, pp. 1377–1390, March 2015.

[12] A. Ahmed, Y. D. Zhang, and J.-K. Zhang, "Coprime array design with minimum lag redundancy," in *Proc. IEEE Int. Conf. Acoustics, Speech, Signal Process. (ICASSP)*, Brighton, UK, May 2019, pp. 4125–4129.

[13] Z. Shi, C. Zhou, Y. Gu, N. A. Goodman, and F. Qu, "Source estimation using coprime array: A sparse reconstruction perspective," *IEEE Sensors J.*, vol. 17, no. 3, pp. 755–765, Feb. 2017.

[14] Z. Zheng, W-Q. Wang, Y. Kong, and Y. D. Zhang, "MISC Array: A new sparse array design achieving increased degrees of freedom and reduced mutual coupling effect," *IEEE Trans. Signal Process.*, vol. 67, no. 7, pp. 1728–1741, April 2019.

[15] A. Ahmed, Y. D. Zhang and B. Himed, "Cumulant-based direction-of-arrival estimation using multiple co-prime frequencies," in *Proc. Asilomar Conf. Signals, Syst. Comput.*, Pacific Grove, CA, Oct. 2017, pp. 1188–1192.

[16] Q. Shen, W. Liu, W. Cui, S. Wu, and P. Pal, "Simplified and enhanced multiple level nested arrays exploiting high-order difference co-arrays," *IEEE Trans. Signal Process.*, vol. 67, no. 13, pp. 3502–3515, July 2019.

[17] A. Ahmed, Y. D. Zhang, and B. Himed, "Effective nested array design for fourth-order cumulant-based DOA estimation," in *Proc. IEEE Radar Conf.*, Seattle, WA, May 2017, pp. 998–1002.

[18] Y. D. Zhang, M. G. Amin, F. Ahmad, and B. Himed, "DOA estimation using a sparse uniform linear array with two CW signals of co-prime frequencies," in *Proc. IEEE Int. Workshop on Comput. Adv. Multi-Sensor Adaptive Process. (CAMSAP)*, Saint Martin, Dec. 2013.

[19] S. Qin, Y. D. Zhang, M. G. Amin, B. Himed, "DOA estimation exploiting a uniform linear array with multiple co-prime frequencies," *Signal Process.*, vol. 130, pp. 37–46, Jan. 2017.

[20] Q. Shen, W. Liu, W. Cui, S. Wu, Y. D. Zhang, and M. G. Amin, "Low-complexity wideband direction-of-arrival estimation based on coprime arrays," *IEEE/ACM Trans. Audio, Speech and Language Process.*, vol. 23, no. 9, pp. 1445–1456, Sept. 2015.

[21] A. Ahmed, D. Silage, and Y. D. Zhang, "High-resolution target sensing using multi-frequency sparse array," in *Proc. IEEE Sens. Array Multichannel Signal Process. Workshop*, Hangzhou, China, June 2020.

[22] S. Zhang, A. Ahmed, Y. D. Zhang, and S. Sun, "DOA estimation exploiting interpolated multi-frequency sparse array," in *Proc. IEEE Sens. Array Multichannel Signal Process. Workshop*, Hangzhou, China, June 2020.

[23] L. Liu, W. Wang, and M. Guo, "Performance analysis for DOA estimation using compressive measurements with coprime frequencies," *IEEE Sensors J.*, vol. 21, no. 6, pp. 8297–8309, March, 2021.

[24] S. Zhang, A. Ahmed, Y. D. Zhang, and S. Sun, "Enhanced DOA estimation exploiting multi-frequency sparse array," *IEEE Trans. Signal Process.*, vol. 69, pp. 5935–5946, 2021.

[25] Y. D. Zhang, M. G. Amin, and B. Himed, "Sparsity-based DOA estimation using co-prime arrays," in *Proce. IEEE Int. Conf. Acoust., Speech, Signal Process. (ICASSP)*, Vancouver, Canada, May 2013.

[26] M. Guo, Y. D. Zhang, and T. Chen, "DOA estimation using compressed sparse array," *IEEE Trans. Signal Process.*, vol. 66, no. 15, pp. 4133–4146, Aug. 2018.

[27] C. Zhou, Y. Gu, Z. Shi, and Y. D. Zhang, "Off-grid direction-of-arrival estimation using coprime array interpolation," *IEEE Signal Process. Lett.*, vol. 25, no. 11, pp. 1710–1714, Nov. 2018.

[28] H. Qiao and P. Pal, "Gridless line spectrum estimation and lowrank Toeplitz matrix compression using structured samplers: A regularization-free approach," *IEEE Trans. Signal Process.,* vol. 65, no. 9, pp. 2221–2236, May 2017.

[29] X. Wu, W.-P. Zhu, and J. Yan, "A Toeplitz covariance matrix reconstruction approach for direction-of-arrival estimation," *IEEE Trans. Veh. Technol.,* vol. 66, no. 9, pp. 8223–8237, Sep. 2017.

[30] C. Zhou, Y. Gu, X. Fan, Z. Shi, G. Mao, and Y. D. Zhang, "Direction-of-arrival estimation for coprime array via virtual array interpolation," *IEEE Trans. Signal Process.,* vol. 66, no. 22, pp. 5956–5971, Nov. 2018.

[31] W. Suleiman, P. Parvazi, M. Pesavento, and A. M. Zoubir, "Non-coherent direction-of-arrival estimation using partly calibrated arrays," *IEEE Trans. Signal Process.*, vol. 66, no. 21, pp. 5776–5788, Nov. 2018.